



**HAL**  
open science

## Electrochemical Stability of the Reconstructed Fe<sub>3</sub>O<sub>4</sub>(001) Surface

Doris Grumelli, Tim Wiegmann, Sara Barja, Finn Reikowski, Fouad Maroun,  
Philippe Allongue, Jan Balajka, Gareth S. Parkinson, Ulrike Diebold, Klaus  
Kern, et al.

► **To cite this version:**

Doris Grumelli, Tim Wiegmann, Sara Barja, Finn Reikowski, Fouad Maroun, et al.. Electrochemical Stability of the Reconstructed Fe<sub>3</sub>O<sub>4</sub>(001) Surface. *Angewandte Chemie International Edition*, 2020, 59 (49), pp.21904-21908. 10.1002/anie.202008785 . hal-03021641

**HAL Id: hal-03021641**

**<https://hal.science/hal-03021641v1>**

Submitted on 4 Dec 2020

**HAL** is a multi-disciplinary open access archive for the deposit and dissemination of scientific research documents, whether they are published or not. The documents may come from teaching and research institutions in France or abroad, or from public or private research centers.

L'archive ouverte pluridisciplinaire **HAL**, est destinée au dépôt et à la diffusion de documents scientifiques de niveau recherche, publiés ou non, émanant des établissements d'enseignement et de recherche français ou étrangers, des laboratoires publics ou privés.

# Electrochemical stability of the reconstructed Fe<sub>3</sub>O<sub>4</sub>(001) surface

Doris Grumelli<sup>1\*</sup>, Tim Wiegmann<sup>2</sup>, Sara Barja<sup>3,4,5</sup>, Finn Reikowski<sup>2</sup>, Fouad Maroun<sup>6</sup>,  
Phillipe Allongue<sup>6</sup>, Jan Balajka<sup>7</sup>, Gareth S. Parkinson<sup>7</sup>, Ulrike Diebold<sup>7</sup>,  
Klaus Kern<sup>8,9</sup>, Olaf M. Magnussen<sup>2</sup>

<sup>1</sup>*Instituto Nacional de Investigaciones Fisicoquímicas Teóricas y Aplicadas, Universidad Nacional de La Plata, La Plata, Argentina*

<sup>2</sup>*Kiel University, Kiel, Germany*

<sup>3</sup>*Departamento de Física de Materiales, Centro de Física de Materiales, University of the Basque Country (UPV/EHU-CSIC), Donostia-San Sebastián, Spain*

<sup>4</sup>*Donostia International Physics Center (DIPC), Donostia-San Sebastián, Spain*

<sup>5</sup>*IKERBASQUE, Basque Foundation for Science, Bilbao, Spain*

<sup>6</sup>*Laboratoire de Physique de la Matière Condensée, CNRS, IP Paris, 91128 Palaiseau, France*

<sup>7</sup>*Institute of Applied Physics, TU Wien, Vienna, Austria*

<sup>8</sup>*Max Planck Institute for Solid State Research, Stuttgart, Germany*

<sup>9</sup>*Ecole Polytechnique Fédérale de Lausanne, Switzerland*

## Abstract

Establishing the atomic-scale structure of metal-oxide surfaces during electrochemical reactions is a key step to modelling this important class of electrocatalysts. Here, we demonstrate that the characteristic  $(\sqrt{2}\times\sqrt{2})R45^\circ$  surface reconstruction formed on (001)-oriented magnetite single crystals is maintained after immersion in 0.1 M NaOH at 0.20 V vs. Ag/AgCl and investigate its dependence on the electrode potential. We follow the evolution of the surface using *in situ* and *operando* surface X-ray diffraction from the onset of hydrogen evolution, to potentials deep in the oxygen evolution reaction (OER) regime. The reconstruction remains stable for hours between -0.20 and 0.60 V and surprisingly, still present at anodic current densities of up to 10 mA/cm<sup>2</sup> and strongly affects the OER kinetics. We attribute this to a stabilization of the Fe<sub>3</sub>O<sub>4</sub> bulk by the reconstructed surface. At more negative potentials, a gradual and largely irreversible lifting of the reconstruction is observed due to the onset of oxide reduction.

Metal oxides have been proposed as an alternative to precious metal electrocatalysts for important technological reactions such as the oxygen reduction reaction (ORR) and the oxygen evolution reaction (OER).<sup>[1]</sup> Obtaining a fundamental understanding of the oxide-electrolyte

interface is crucial for modelling electrochemical reactions and optimizing catalyst design, but determining the atomic scale structure by *in situ* and *operando* techniques is challenging, and many oxides are thought to be unstable under reaction conditions.

Magnetite ( $\text{Fe}_3\text{O}_4$ ) single crystals, especially in their (001) orientation, are an ideal model system to study the electrochemical properties of metal oxides because they are electrically conductive and the surface structure is precisely known.<sup>[2]</sup> Following ultrahigh vacuum (UHV) preparation, the surface adopts a  $(\sqrt{2}\times\sqrt{2})\text{R}45^\circ$  reconstruction characterized by undulating rows of Fe cations in scanning tunneling microscopy (STM) images. The subsurface cation vacancy (SCV) model established for this reconstruction is supported by quantitative low energy electron diffraction (LEED)<sup>[2]</sup> and surface X-ray diffraction (SXRD) results,<sup>[3]</sup> as well as the STM data and density functional theory (DFT) calculations.<sup>[2]</sup> The surface is stabilized by a combination of subsurface Fe vacancies and interstitials, and the surface atoms relax toward the nearest interstitial Fe atom ( $\text{Fe}_{\text{int}}$ ) in the second layer.<sup>[2]</sup> This produces the periodic lattice distortion and the  $(\sqrt{2}\times\sqrt{2})\text{R}45^\circ$  superstructure (Fig. 1a,b). The surface reconstruction is oxidised with respect to bulk  $\text{Fe}_3\text{O}_4$ , with all cations in the outermost 4 atomic layers being  $\text{Fe}^{3+}$ .<sup>[2]</sup>

While the structure of  $\text{Fe}_3\text{O}_4(001)$  is well known in UHV, it is not clear whether the surface changes in aqueous solution. Atomic force microscopy (AFM) studies have shown that the nanoscale morphological appearance of  $\text{Fe}_3\text{O}_4(001)$  is maintained in an electrochemical environment,<sup>[4]</sup> but recent work suggests the reconstruction is lifted by exposure to 6 mbar water vapour, as well as by pure liquid water at pH 7.<sup>[5]</sup> This is in line with previous surface X-ray diffraction measurements, which also found the reconstruction to be lifted by water vapour.<sup>[3]</sup> In this work, we demonstrate that this problem can be overcome if the electrochemical conditions at the interface are properly controlled, and that the stability range of the surface reconstruction extends well into the OER regime.

Following procedures reported in the literature,<sup>[2]</sup> we prepared an  $\text{Fe}_3\text{O}_4(001)$  single crystal with a  $(\sqrt{2}\times\sqrt{2})\text{R}45^\circ$  surface reconstruction. STM images of the crystal obtained at room temperature directly after UHV preparation (Fig. 1c,d) show well-ordered surfaces with extended, atomically-smooth terraces, and reveal the undulating rows of surface Fe atoms running in the  $\langle 110 \rangle$  directions.<sup>[2]</sup> The measured LEED pattern (Fig. 1e) exhibits the expected  $(\sqrt{2}\times\sqrt{2})\text{R}45^\circ$  symmetry. STM images acquired after 5 minutes exposure to air (Fig. 1f,g) show that the characteristic undulating rows of Fe atoms are still present, although they are partly obscured by residual adsorbates. The LEED pattern also continues to exhibit the  $(\sqrt{2}\times\sqrt{2})\text{R}45^\circ$

superstructure (Fig. 1h), suggesting the reconstruction at least partially survives brief air exposure.

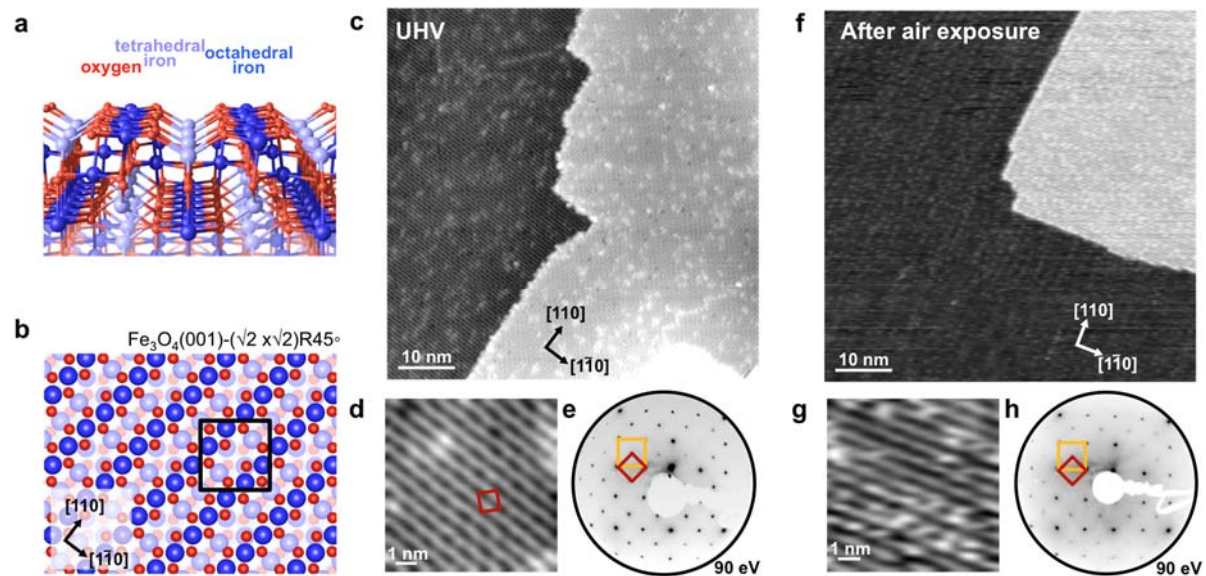


Figure 1. a) Perspective view and b. top view of the subsurface cation vacancy model of the reconstructed  $Fe_3O_4(001)$  surface. In-plane relaxations perpendicular to the surface octahedral Fe (dark blue) row direction lead to a  $(\sqrt{2} \times \sqrt{2})R45^\circ$  symmetry (black square). STM images and LEED of c-e) the reconstructed  $Fe_3O_4(001)$  surface prepared under ultra-high vacuum and f-h) the  $Fe_3O_4$  sample from b after 5 min exposure to air.  $(\sqrt{2} \times \sqrt{2})R45^\circ$  and  $(1 \times 1)$  unit cells are indicated by red and yellow squares, respectively.

To probe the surface structure *in situ*, we performed SXRD measurements. Here, the UHV-prepared  $Fe_3O_4(001)$  sample was immersed into an Ar-saturated, 0.1 M NaOH electrolyte at a potential of 0.20 V. Based on cyclic voltammograms (CVs), this potential is in the middle of an extended (pseudo-) capacitive region, and well positive of the potential where reduction of the sample to  $Fe(OH)_2$  commences (Fig. S1). The SXRD measurements reveal the  $Fe_3O_4(001)$  crystal truncation rods (CTRs, indicated by squares in the scheme in Fig. 2a) as well as additional rods at the characteristic positions of a  $(\sqrt{2} \times \sqrt{2})R45^\circ$  superstructure (circles). The in-plane full width at half maximum of these superstructure peaks is in the range of  $0.1$  to  $0.4^\circ$  (Fig. 2b and Fig. S2), which is comparable to that of the CTRs, indicating extended reconstruction domains. The intensity of these superstructure rods varies along the surface-normal direction by only a factor of  $\approx 10$  (Fig. 2b, right), as expected for a quasi-two-dimensional structure, and in good qualitative agreement with what was found for reconstructed  $Fe_3O_4(001)$  surfaces under UHV conditions.<sup>[3]</sup>

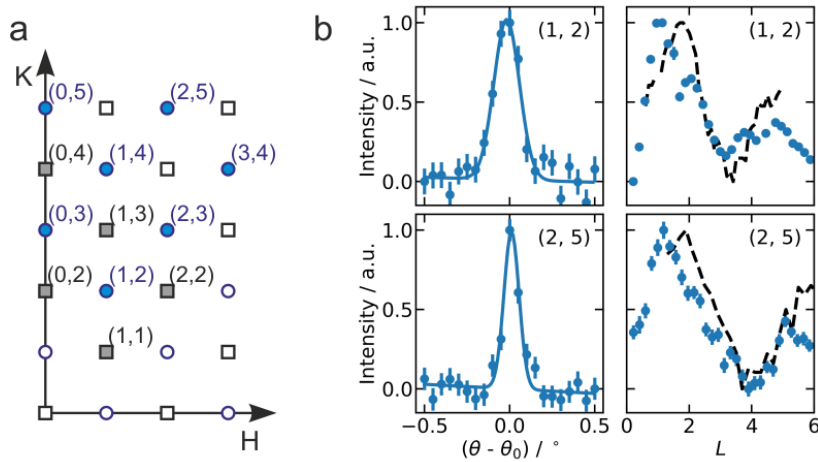


Figure 2. a) Scheme of the  $\text{Fe}_3\text{O}_4(001)$  in-plane reciprocal space geometry, showing the position of the CTRs (black squares) and  $(\sqrt{2} \times \sqrt{2})\text{R}45^\circ$  superstructure rods (blue circles). Measured rods are indicated by filled symbols. b) Azimuthal scan at  $L=1.3$  (left) and  $L$  dependence of (1,2) and (2,5) superstructure rod (right), obtained in 0.1 M NaOH at 0.20 V (blue), compared to those of reconstructed  $\text{Fe}_3\text{O}_4(001)$  under UHV conditions (black dashed lines, taken from Ref. 3).<sup>[3]</sup>

These data provide clear evidence that the  $(\sqrt{2} \times \sqrt{2})\text{R}45^\circ$  reconstruction, formed under UHV conditions, is maintained on the  $\text{Fe}_3\text{O}_4(001)$  electrode surface at 0.20 V. Indeed, our experiments show that it is stable for many hours over the range -0.20 to 0.60 V. To monitor changes in the  $\text{Fe}_3\text{O}_4(001)$  surface reconstruction over a wider potential range, the intensity of the superstructure (1, 2) rod at  $L=1.3$  was recorded during CVs and potential step experiments. First, we discuss the behaviour in the negative potential range. Fig. 3 shows the electrochemical current (black) together with the simultaneously-obtained superstructure intensity at (0,3,0.5) (blue) during a potential cycle from 0.20 to -0.90 V and back at 2 mV/s. The (0,3,0.5) intensity in the negative sweep is constant down to -0.20 V. Below this potential, the intensity gradually decreases until the peak completely disappears at about -0.80 V. A similar change of the reconstruction rod intensity with potential was found in an experiment where the reconstruction was lifted by 10 s long potential pulses from 0.2 V to successively more negative potentials (Fig. S3). This demonstrates that the gradual lifting of the reconstruction is not a kinetic effect, but reflects a genuine potential dependence. That the lifting of the reconstruction proceeds quickly is also directly visible in potential step experiments to -0.80 V (Fig. S3, inset).

In the reverse potential sweep of the CV in Fig. 3, the reconstruction peak slightly recovers above -0.30 V, leading to an integrated intensity that is  $\approx 10\%$  of the value before the potential cycle at 0.20 V (see Fig. S4). These observations indicate that the cathodic electrochemical lifting of the reconstruction can be reversed to a small extent at positive potentials, somewhat akin to the potential-dependent reconstruction behaviour of metal surfaces.<sup>[6]</sup> Overall, however, this lifting is largely irreversible. Even after the potential was kept for extended time periods at 0.20 V the reconstruction did not show any significant further increase. A full recovery of the surface reconstruction after its electrochemical lifting was only possible by sputtering and annealing in UHV.

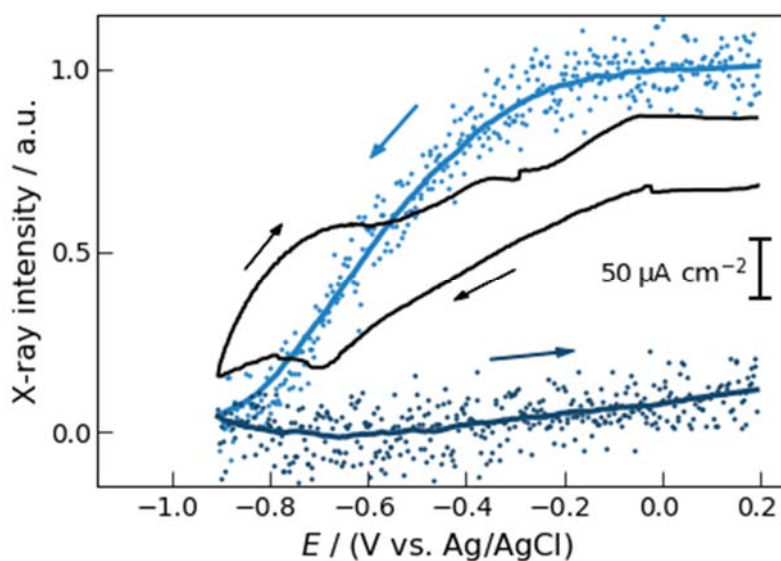


Figure 3. Relative change of X-ray intensity at (0,3,0.5) (blue) and simultaneously measured electrochemical current density (black) during a potential cycle from 0.20 to -0.90 V at 2 mV/s.

The  $\text{Fe}_3\text{O}_4(001)$  CTRs exhibit minor changes during the lifting of the reconstruction, suggesting that the latter is a pure surface phase transition and does not involve substantial restructuring or roughening of the surface. This is in agreement with recent *ex situ* AFM observations of  $\text{Fe}_3\text{O}_4(001)$  emerged from an electrochemical environment.<sup>[4]</sup> However, pronounced irreversible roughening occurs after changing the potential to even more negative values of  $\leq -1.20$  V, where reduction of the Fe oxide to  $\text{Fe}^0$  commences (Fig. S5).<sup>[7]</sup>

In contrast to the behaviour at negative potentials, the reconstruction is remarkably stable at potentials where oxygen evolution commences. Potential cycles into this regime show only minor changes in the intensity of the reconstruction rods (Fig. 4). Furthermore, the intensity only slightly decays with time if the sample is kept deep in the OER regime (Fig. S6 and S7), even at OER overpotentials  $>600$  mV where the current density is close to the benchmark value

of  $10 \text{ mA/cm}^2$  commonly used in OER catalyst characterization.<sup>[1d]</sup> This suggests that the OER can proceed on the reconstructed surface without strongly affecting the local surface structure. On the other hand, the presence of the reconstruction clearly affected the OER kinetics. Although the OER current for both reconstructed and unreconstructed  $\text{Fe}_3\text{O}_4(001)$  increases with the same Tafel slope of  $\approx 70 \text{ mV/decade}$ , which is a typical value for spinel-type oxides in alkaline solution [enter Ref. Q. Zhao, Z. Yan, C. Chen, J. Chen, Spinel: Controlled Preparation, Oxygen Reduction/Evolution Reaction Application, and Beyond. *Chem. Rev.* **117**, 10121-10211 (2017).], OER on the reconstructed surface starts at more negative potentials (Fig. 4, dashed line). This suggests that the reaction occurs on both surfaces via the same mechanism but that the number or activity of the OER reaction sites is higher on the reconstructed surface. The smaller OER overpotential of the reconstructed surface might be caused by the distinct defect structure associated with the  $(\sqrt{2}\times\sqrt{2})\text{R}45^\circ$  reconstruction, specifically the presence of surface vacancies. For  $\text{Fe}_2\text{O}_3$ , DFT calculations predicted large shifts of the OER in the presence of Fe or oxygen vacancies.<sup>[10]</sup> Whether the same effect occurs for reconstructed  $\text{Fe}_3\text{O}_4(001)$  remains to be clarified, however.

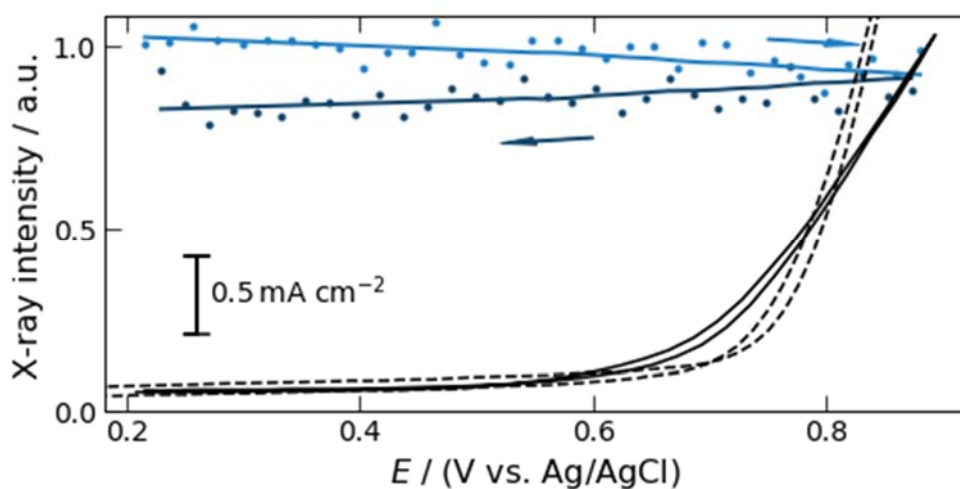


Figure 4. X-ray intensity (blue) at (0,3,0.5) and simultaneously recorded electrochemical current (black solid line) showing the stability of the  $(\sqrt{2}\times\sqrt{2})\text{R}45^\circ$  reconstruction deep in the OER regime. The potential was corrected for the electrolyte resistance; arrows indicate scan direction ( $20 \text{ mV/s}$ ). Dashed black lines shown a corresponding CV of an unreconstructed  $\text{Fe}_3\text{O}_4(001)$  surface, prepared by a potential excursion to  $-1.2 \text{ V}$ .

In the following, we will show that our observations can be explained by considering the atomic-scale structure of the  $(\sqrt{2}\times\sqrt{2})\text{R}45^\circ$  reconstruction. Previously, it was reported that the



reconstruction was lifted almost instantly following exposure of the reconstructed surface to atomic hydrogen, formic acid, water vapour, liquid water, and neutral electrolyte without potential control.<sup>[8]</sup> One key link between these prior experiments is the extensive hydrogenation of the surface oxygen lattice that occurs through the deprotonation of molecular adsorbates. Since we do not observe lifting of the reconstruction in strongly alkaline electrolyte at 0.20 V, we surmise that this mechanism does not occur. As will be shown below, this can be rationalized by considering the electrochemical equilibria that determine the amount of hydroxylation in that environment.

We first discuss the stability of the reconstruction over a wide potential regime, which at first glance appears surprising. According to thermodynamic data (supporting information), bulk Fe<sub>3</sub>O<sub>4</sub> is only stable in a narrow potential window from about -1.05 to -0.81 V at pH 13. Reductive conversion into metallic Fe is expected at more negative potentials, while oxidative conversion to an Fe(III) oxide (FeOOH or Fe<sub>2</sub>O<sub>3</sub>) is expected at more positive potentials. We attribute the remarkable structural stability of Fe<sub>3</sub>O<sub>4</sub>(001) above -0.20 V to the unique near surface structure of the SCV reconstruction, where all Fe in the outermost 4 atomic layers are already in a fully oxidized Fe<sup>3+</sup> state.<sup>[2]</sup> These first four layers act as a passivating film, which is capable of protecting the bulk material from further oxidation. Considering the prevalent OER reaction mechanisms for oxides in alkaline solution (supporting information, Fig. S9), this surface will remain in this state, i.e., be almost fully terminated by oxygen atoms, even during O<sub>2</sub> evolution.

*Vice versa*, the lifting of the ( $\sqrt{2}\times\sqrt{2}$ )R45° reconstruction between -0.20 and -0.80 V can be attributed to the cathodic reduction of Fe<sup>3+</sup> into Fe<sup>2+</sup> surface sites within this Fe(III) oxide and the concomitant hydroxylation of the magnetite surface (see eq. S4). The reaction is associated with a cathodic current in the CV peaking at -0.68 V. This interpretation is well supported by *in situ* Raman studies of passive films, which showed that the reduction of Fe(III) oxide into Fe(II)/Fe(III) oxide starts around -0.5 V in 0.1 M NaOH.<sup>[7b]</sup> It is also in agreement with DFT calculations for similar electrode materials, such as Fe<sub>2</sub>O<sub>3</sub> and CoOOH, which indicated that surface hydroxylation occurs gradually over a wide potential range and can start more than 0.5 V positive of the phase transition to the bulk hydroxides.<sup>[9]</sup> Such behavior could also account for a potential-dependent replacement of reconstructed O-terminated with unreconstructed OH-terminated surface areas on Fe<sub>3</sub>O<sub>4</sub>(100).

Finally, our results highlight the importance of potential control in studies of such model oxide catalysts. While the Fe<sub>3</sub>O<sub>4</sub>(001) reconstruction is gradually lifted as soon as the potential is approaching the Fe<sup>3+</sup> reduction reaction, it is stable at sufficiently oxidizing potentials. These



stable conditions must be applied during sample immersion to maintain the surface structure. If the sample is at open circuit potential (OCP), this can be achieved by an oxidising environment, e.g. dissolved O<sub>2</sub> (see Fig. S8), even without external potential control. This explains why exposure to pure water vapour or clean, O<sub>2</sub>-free water was found to lift the Fe<sub>3</sub>O<sub>4</sub>(001) reconstruction,<sup>[3]</sup> whereas transfer of the sample through (moist) air can preserve it.

In conclusion, this work demonstrates that electrochemical studies of well-defined oxide single crystal electrodes are possible by combining sample preparation in UHV with structure-sensitive *in situ / operando* methods. Under suitable transfer conditions, specifically at high pH and electrochemical controlled potential, the ( $\sqrt{2} \times \sqrt{2}$ )R45° surface reconstruction of Fe<sub>3</sub>O<sub>4</sub>(001) can be maintained and is even stable deep in the OER regime. The latter suggests that the fully oxidized nature of the reconstructed surface protects the Fe<sub>3</sub>O<sub>4</sub> bulk against further oxidation. This opens up new possibilities for mechanistic studies of structurally highly defined oxide model surfaces in electrochemical environment, including the derivation of structure-activity relationships for oxide electrocatalysts, to which the results presented above are a first step. In particular, it enables future “single-atom” catalysis studies for which isolated metal adatoms on the reconstructed Fe<sub>3</sub>O<sub>4</sub>(001) surface provides a unique model system.<sup>[11]</sup> Just as for gas phase catalysis, model systems with well-defined active site structure offer unique opportunities to obtain a deeper understanding of OER/ORR surface reaction mechanisms.

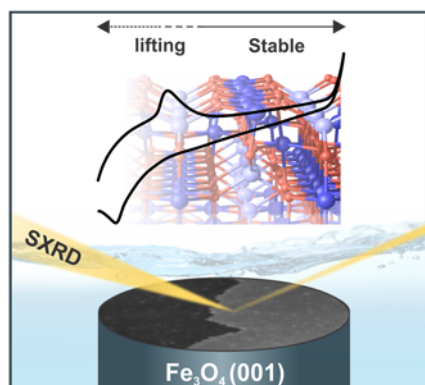
## ACKNOWLEDGMENT

We gratefully acknowledge financial support by AGENCIA PICT 20141415 and 2016069, EC-MEC (ANR-15-CE30-0024-01 and DFG-Ma1618/2020), European Research Council - European Union’s Horizon 2020 (864628), Austrian Science Fund FWF (Project Z-250 Wittgenstein Prize), and RyC program RYC-2017-21931 and Basque Government Project (IT-1255-19). We thank the ESRF for the PhD fellowship for TW and the ID03 beamline staff, in particular H. Isern.

## REFERENCES

- [1] a) A. Bergmann, T. E. Jones, E. Martinez Moreno, D. Teschner, P. Chernev, M. Gliech, T. Reier, H. Dau, P. Strasser, *Nat. Catal.* **2018**, *1*, 711-719; b) M. P. Browne, Z. Sofer, M. Pumera, *Energy Environ. Sci.* **2019**, *12*, 41-58; c) E. Fabbri, T. J. Schmidt, *ACS Catal.* **2018**, *8*, 9765-9774; d) C. C. L. McCrory, S. Jung, J. C. Peters, T. F. Jaramillo, *J. Am. Chem. Soc.* **2013**, *135*, 16977-16987.
- [2] R. Bliem, E. McDermott, P. Ferstl, M. Setvin, O. Gamba, J. Pavelec, M. A. Schneider, M. Schmid, U. Diebold, P. Blaha, L. Hammer, G. S. Parkinson, *Science* **2014**, *346*, 1215.

- [3] B. Arndt, R. Bliem, O. Gamba, J. E. S. van der Hoeven, H. Noei, U. Diebold, G. S. Parkinson, A. Stierle, *Surf. Sci.* **2016**, *653*, 76-81.
- [4] M. Müllner, M. Riva, F. Kraushofer, M. Schmid, G. S. Parkinson, S. F. L. Mertens, U. Diebold, *J. Phys. Chem. C* **2019**, *123*, 8304-8311.
- [5] F. Kraushofer, F. Mirabella, J. Xu, J. Pavelec, J. Balajka, M. Müllner, N. Resch, Z. Jakub, J. Hulva, M. Meier, M. Schmid, U. Diebold, G. S. Parkinson, *J. Phys. Chem.* **2019**, *151*, 154702.
- [6] D. M. Kolb, *Angew. Chem. Int. Ed.* **2001**, *40*, 1162-1181.
- [7] a) P. Allongue, S. Joiret, *Phys. Rev. B Condens. Matter* **2005**, *71*, 115407; b) S. Joiret, P. Allongue, in *Passivation of Metals and Semiconductors, and Properties of Thin Oxide Layers* (Eds.: P. Marcus, V. Maurice), Elsevier Science, Amsterdam, **2006**, pp. 89-94.
- [8] a) O. Gamba, H. Noei, J. Pavelec, R. Bliem, M. Schmid, U. Diebold, A. Stierle, G. S. Parkinson, *J. Phys. Chem. C* **2015**, *119*, 20459-20465; b) G. S. Parkinson, N. Mulakaluri, Y. Losovyj, P. Jacobson, R. Pentcheva, U. Diebold, *Phys. Rev. B Condens. Matter* **2010**, *82*, 125413.
- [9] a) J. Noh, H. Li, O. I. Osman, S. G. Aziz, P. Winget, J.-L. Brédas, *Adv. Energy Mater.* **2018**, *8*, 1800545; b) J. Chen, A. Selloni, *J. Phys. Chem. C* **2013**, *117*, 20002-20006.
- [10] a) X. Zhang, P. Klaver, R. van Santen, M. C. M. van de Sanden, A. Bieberle-Hütter, *J. Phys. Chem. C* **2016**, *120*, 18201-18208; b) M.-T. Nguyen, S. Piccinin, N. Seriani, R. Gebauer, *ACS Catal.* **2015**, *5*, 715-721.
- [11] a) Z. Jakub, J. Hulva, M. Meier, R. Bliem, F. Kraushofer, M. Setvin, M. Schmid, U. Diebold, C. Franchini, G. S. Parkinson, *Angew. Chem. Int. Ed.* **2019**, *58*, 13961-13968; b) Z. Jakub, J. Hulva, F. Mirabella, F. Kraushofer, M. Meier, R. Bliem, U. Diebold, G. S. Parkinson, *J. Phys. Chem. C* **2019**, *123*, 15038-15045; c) Z. Novotný, G. Argentero, Z. Wang, M. Schmid, U. Diebold, G. S. Parkinson, *Phys. Rev. Lett.* **2012**, *108*, 216103.



In situ and operando X-ray diffraction shows that the surface reconstruction of magnetite single crystals, formed in vacuum, persists under harsh oxygen evolution reaction conditions and protects the bulk magnetite from further oxidation. It also alters the catalytic properties with respect to the unreconstructed surface. The reconstruction is irreversibly lifted upon reduction of surface iron cations.

**KEYWORDS.** Oxide surface structure – electrocatalysis - Oxygen evolution reaction - Magnetite single crystal - Operando X ray surface diffraction